WEP Warwick Evans Publishing

International Journal of Materials Science and Technology Studies

ISSN: 3006-7693 (Print), ISSN: 3006-3744 (Online) | Volume 3, Number 1, Year 2025
DOI: https://doi.org/10.62051/ijmsts.v3n1.01
Journal homepage: https://wepub.org/index.php/IJMSTS/index

Molecular Dynamics Simulation on the Frictional Behavior and Mechanisms of Graphene, Boron Nitride and Their Doping Structures

Zhangchao Li *

Faculty of Civil Engineering and Mechanics, Jiangsu University, Zhenjiang, China

ABSTRACT

By establishing a boron nitride-doped graphene system and using molecular dynamics simulation to measure and characterize its frictional behavior, it was found that the doping of boron nitride significantly affects the friction behavior of graphene. this study focuses on the outer layer of pinned atoms on the indenter that have a decisive influence on the friction performance and calculates the resistance of such atoms during the sliding process of the indenter. In addition to the van der Waals cohesive energy, the deformation of the 2D film near the pinned atoms is also studied. The results show that boron nitride doping not only reduces the friction resistance of graphene, but also changes the friction peak value from a basically constant state to a large amplitude and long-period oscillation. Here, changes in the frictional properties and behavior of the doped graphene can be attributed to higher cohesive energy between boron nitride and the indenter, lower adhesion/frictional resistance, and lower strain of the doped graphene around the pinned atoms.

KEYWORDS

Frictional behavior; Graphene; Hexagonal boron nitride (h-BN); Doping

1. INTRODUCTION

Recognized as an inherent phenomenon in mechanical systems, friction is the main cause of energy dissipation and device loss. The traditional lubrication method is generally to reduce the friction coefficient of the contact surface by introducing an external lubricant into the contact surface. As mechanical systems and electronic components continue to miniaturize, lubricants have proven to be no longer suitable under extreme conditions or at the nanoscale. Therefore, it is crucial to seek and investigate new lubrication systems at the nanoscale [1, 2]. As a typical representative of two-dimensional materials, graphene has excellent mechanical robustness, chemical stability and electromagnetic properties, and is considered to be an ideal candidate material for forming low-friction interfaces [3-7]. In various fields such as advanced nanoelectronic devices [8, 9], and nanolubricating coatings on engineering surfaces [10-14], the material is expected to have great application prospects.

To deeply investigate the friction of two-dimensional materials at the nanoscale and improve the control over friction stability, researchers have extensively explored the friction properties of low-friction interfaces represented by graphene, identifying the main influences on friction and attempting to unravel the physical mechanisms behind them. Previous studies have shown that graphene has thickness-related friction dependence, with out-of-plane deformation being the main influencing factor. Meanwhile, the roughness level of the interface and the presence of defects also have a significant influence on the friction behavior.

In addition to graphene, hexagonal boron nitride (h-BN) is also a two-dimensional material with excellent lubrication properties. The crystal structure of h-BN is a hexagonal crystal system, consisting of boron (B) and nitrogen (N) atoms. Its structure is similar to graphene, but the boron and nitrogen atoms are arranged in the shape of a hexagonal honeycomb in BNBN, forming a planar layered structure. In recent years, research on the friction properties of graphene and h-BN has mainly focused on various aspects such as the super-slippery interface, the number of layers, the bonding with the substrate, and the influence of surface groups. For example, Zheng et al [15] found that ultra-low friction of graphene can be achieved through moiré lattice mismatch. Leven et al [16] investigated the sliding behavior of graphene on an h-BN surface, and the result showed that sufficiently large graphene films will exhibit stable supersliding behavior when sliding on the surface of h-BN. Regarding the study of chemical modification on graphene friction, current researchers have mainly investigated the effect of surface groups such as H, F, and hydroxyl groups on the friction behavior of graphene. Recently, Nataly Herrera-Reinoza et al [17] successfully prepared h-BNC, described as h-BN doped graphene, by chemical vapor deposition. The research reported its unique electronic properties and predicted that the band gap value could be controlled by fine-tuning growth conditions and substrate optimization. Due to its predictable semiconductor properties, this h-BNC is expected to have great application prospects in the fields of nanoelectronics [18, 19], nanophotonics devices [20], photocatalytic activity [21], gas adsorption [22] and supercapacitors [23]. Based on the above findings, this study explored the friction behavior of the in-plane heterojunction system of h-BN-doped graphene.

2. METHOD

Based on the LAMMPS simulation software, this study realized the physical process of using a rigid bowl-shaped silicon indenter to simulate AFM to measure the friction signal of the graphene system. For the indenter, a virtual spring was used to connect the virtual silicon block in the X and Y directions to apply normal pressure and moving speed, respectively, to perform scanning. In the X direction, the indenter is subjected to lateral force from graphene during the scanning process, which is transmitted to the virtual block through the spring. The reaction force on the virtual block is calculated and collected, and is identified as the friction force on the AFM from graphene. The NVT ensemble was selected for this simulation, the time step was 1fs, and the temperature was 300K. The interatomic interaction potentials were selected as follows: SW potential was used between silicon atoms, Tersoff potential was used between carbon atoms and between h-BN, and L-J potential was used to describe the interlayer van der Waals interaction.

In the double-layer graphene system based on AB stacking (Figure 1(a)), the upper graphene layer is doped with a h-BN structure with a size of 3.6 nm*3.6 nm (Figure (1b)), and boron (B) and nitrogen (N) atoms are represented by purple and gray, respectively. In the system, the silicon crystal uses (100) silicon ordering, the unit cell is a cubic unit cell with a size of 39 nm*32 nm and a thickness of 2 nm. The silicon substrate is divided into an upper free layer and a lower fixed layer, and the graphene directly contacts the upper free layer. A spherical crystalline silicon (Si) tip with a radius of 8 nm was used to simulate sliding friction force measurements under an atomic force microscope (AFM). The rigid tip was used to eliminate the contribution of tip deformation to friction so as to clearly extract the trend of interface friction behavior [24]. The size of graphene is 35 nm*28 nm, and the interlayer thickness is 0.335 nm. The spring stiffnesses were chosen to be 32 N/m and 1.6 N/m, respectively, the scanning speed was 5 m/s, and the normal force was 3 nN. Furthermore, the mass of the tip atom was artificially reduced by a factor of ten to enhance oscillation damping and reduce fluctuations in the measured signal.

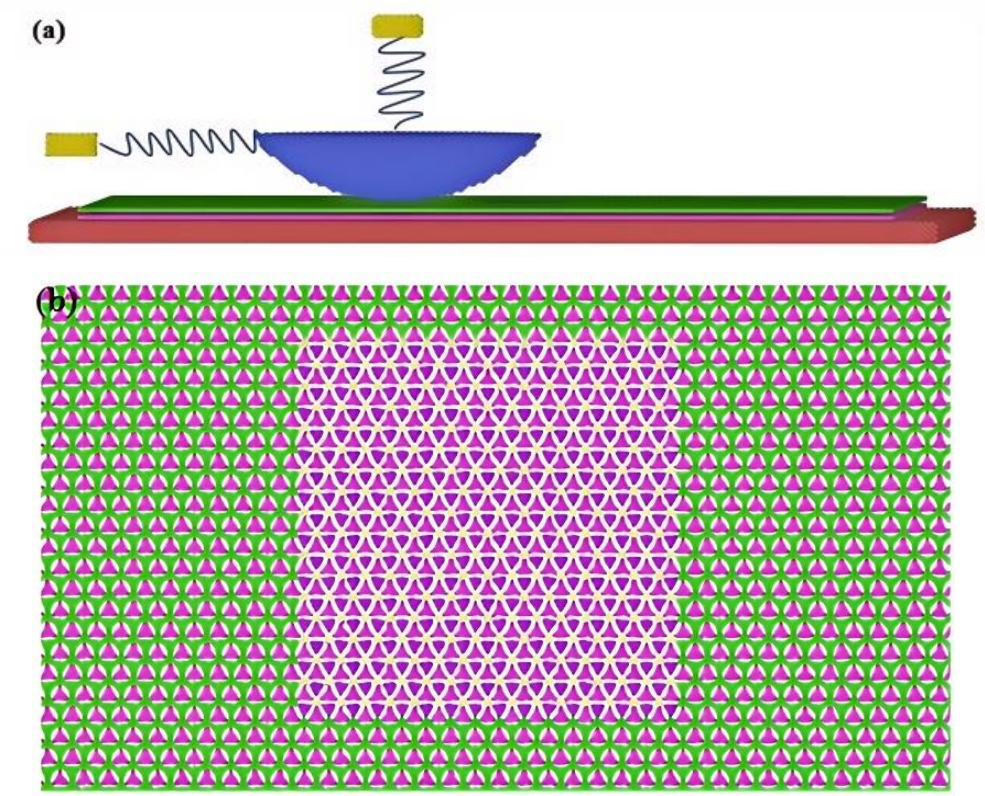

Figure 1. (a) Schematic mode of MD simulation, (b) structures of h-BN doped graphene

In the double-layer graphene system based on AB stacking (Figure 1(a)), the upper graphene layer is doped with a h-BN structure with a size of 3.6 nm*3.6 nm (Figure 1b), and boron (B) and nitrogen (N) atoms are represented by purple and gray, respectively. In the system, the silicon crystal uses (100) silicon ordering, the unit cell is a cubic unit cell with a size of 39 nm*32 nm and a thickness of 2 nm. The silicon substrate is divided into an upper free layer and a lower fixed layer, and the graphene directly contacts the upper free layer. A spherical crystalline silicon (Si) tip with a radius of 8 nm was used to simulate sliding friction force measurements under an atomic force microscope (AFM). The rigid tip was used to eliminate the contribution of tip deformation to friction so as to clearly extract the trend of interface friction behavior [24]. The size of graphene is 35 nm*28 nm, and the interlayer thickness is 0.335 nm. The spring stiffnesses were chosen to be 32 N/m and 1.6 N/m, respectively, the scanning speed was 5 m/s, and the normal force was 3 nN. Furthermore, the mass of the tip atom was artificially reduced by a factor of ten to enhance oscillation damping and reduce fluctuations in the measured signal.

3. RESULTS AND DISCUSSION

Based on the doped system, the results obtained show (Figure 2) that the friction behavior under the doped system conforms to the stick-slip curve, and the period is close to that of pure graphene. This indicates that doping h-BN into graphene does not bring about significant distortion of its lattice structure, because the lattice structure of h-BN is the same as that of graphene and the lattice constant is similar. From the overall friction performance, the friction peak value (4nN) of the doped system is smaller than the friction peak value (5nN) of the pure graphene system, and the average friction value is also smaller than the average value of the pure graphene system. Such a result shows that the in-plane doping method contributes to reducing the friction of graphene and optimizing the lubrication performance of graphene. In addition to the changes in friction performance, the friction behavior observed in molecular simulations is also entirely different from that of pure graphene. As shown in Figure 2(b), as the indenter scans from the graphene area to the doped area, the friction force continues to decrease. When the indenter is completely in the scanning area, the friction force

is the smallest, and then the friction force gradually increases as the indenter slowly leaves the scanning area. In general, the friction force shows a trend of rising, falling, and then rising again, which is significantly different from the almost stable behavior of the friction peak values of pure graphene and h-BN films. Especially in the first stage, the friction force increase behavior occurs in the graphene area, which is consistent with the strengthening behavior in the initial stage of friction reported by Suzhi Li et al [24].

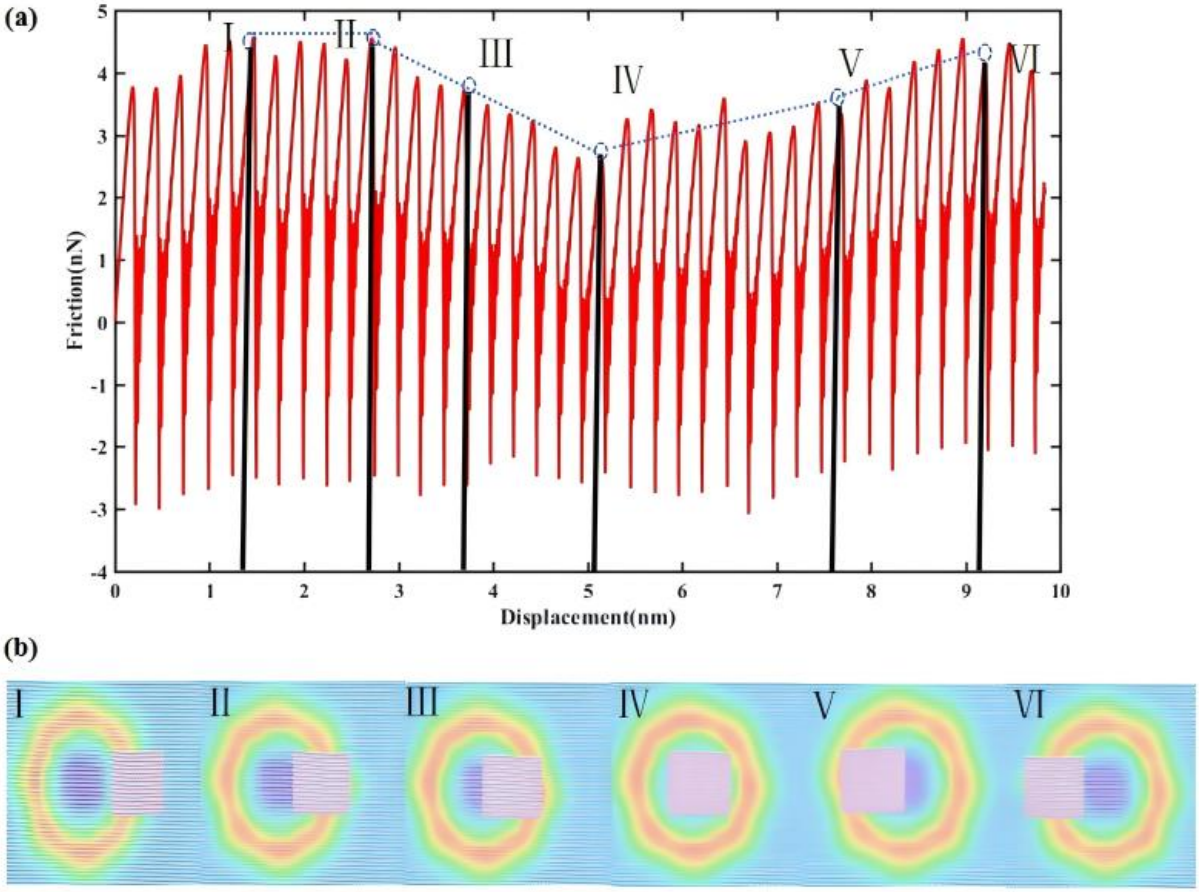

Figure 2. (a) Friction-displacement curve of the doped system along with the annotated special moments and (b) the tip position corresponding to the special moments

To investigate the special behavior of the periodic change of friction force of doped graphene, six points on the friction displacement curve are marked in Figure 2(a), namely I-VI, and their corresponding indenter positions are marked in Figure 2(b). From left to right, they are (I) the indenter is placed in the graphene area, (II) the indenter just touches the doped area, (III) the indenter touches half of the doped area, (IV) the indenter completely touches the doped area, (V) the indenter leaves the doped area and (VI) the indenter completely leaves the doped area. Since graphene will be adsorbed onto the indenter when it is scanned on graphite, the graphene indentation in the Y direction is rendered to represent the position of the indenter, i.e., the blue indentation in Figure 2(b). By comparing Figure 2(a) and (b), it can be seen that the increase in friction in the initial (graphene) transition area (before position I) is the result of the adjustment of the graphene film and the improvement of the adhesion quality of the indenter. In the doping system, when the indenter moves from the graphene area to the doping area (regions II to III), the friction decreases; when the indenter completely covers the doping area (IV), the friction goes to the lowest; when the indenter leaves the doping area and returns to the graphene area (regions V to VI), the friction rises again.

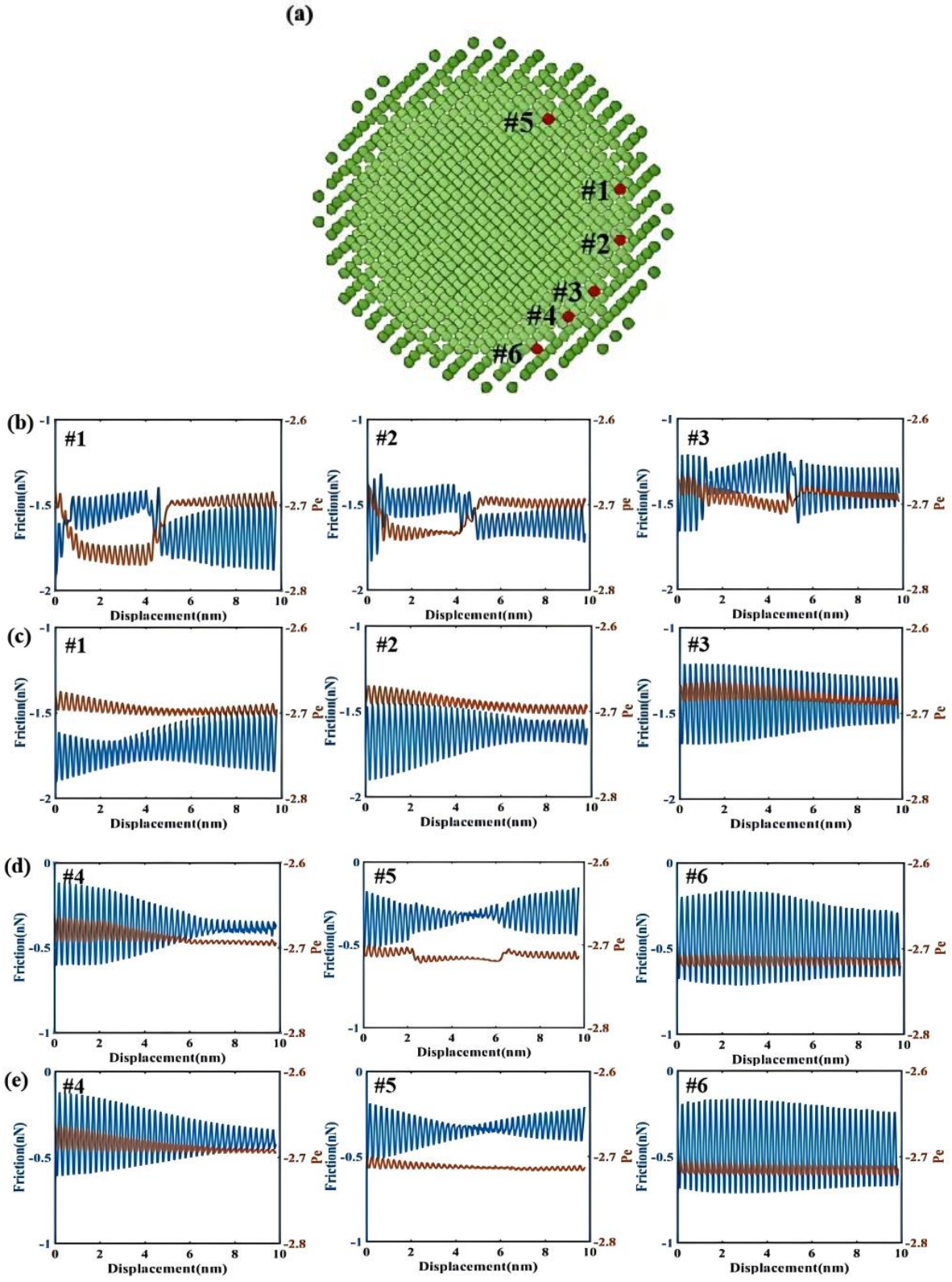

Figure 3. (a) Selection of the tip atoms subjected to external force, (b) and (d) force and energy changes of the selected atoms in doped system and (c) and (e) force and energy changes in the graphene system

To explore the change of friction caused by doping from the perspective of the force on the atoms of the indenter, Figure 3(a) shows the atomic force distribution before the indenter starts scanning. On the indenter, atoms are subjected to forces in two directions. The red represents the thrust exerted on atoms during the sliding of the indenter, and the blue represents the friction resistance exerted on

atoms during the indenter process. The study focused on the atoms that are subject to frictional resistance and regards them as local pinning atoms, which are important because they are the source of friction force generation during the sliding of the indenter.

Figure 3(a) shows the six selected atoms that are subject to the largest lateral friction resistance, and the atoms are distributed at different positions on the outer surface of the indenter. Figures 3(b), (c), (d) and (e) respectively reflect the changes in the lateral force and potential energy exerted on the six selected atoms in the pure graphene system and the h-BN-doped graphene system when the indenter is scanned along the X direction, where the blue line represents the lateral force (fx) and the red line represents the potential energy (pe). The calculation results show that in the pure graphene system and the doped system, the lateral friction resistance and potential energy of the selected atoms show different change trends. (1) In the doping system, the changes of atoms #1-#3 are the most obvious. From the initial high friction to low friction, it finally presents a stable state of high friction; its corresponding potential energy also presents the same trend of change, from the initial high potential energy state to the low potential energy state, and finally stabilizes in the high potential energy state. While the changes in force and potential energy of atoms #4-#6 are not obvious. (2) The force changes and potential energy of atoms in the graphene system show a relatively stable state, with no obvious changes. During the scanning process of the indenter, the potential energy reflects the strength of the interaction between atoms. High potential energy indicates strong interaction, while low potential energy indicates weak interaction. Therefore, the effect of doping is manifested in that during the scanning process, the pinning state of the pinned atoms in the doped area is weaker than that in the graphene area, the friction resistance it encounters is lower, and the interaction between atoms is also weak. These observations explain the main reason why friction becomes lower in the doped regions and stronger in the graphene regions in the doped system. Changes in atomic forces and energy have been shown to be one of the reasons for the periodic reduction in friction in the doped system. As mentioned earlier, doping also changes the evolution of the graphene interface.

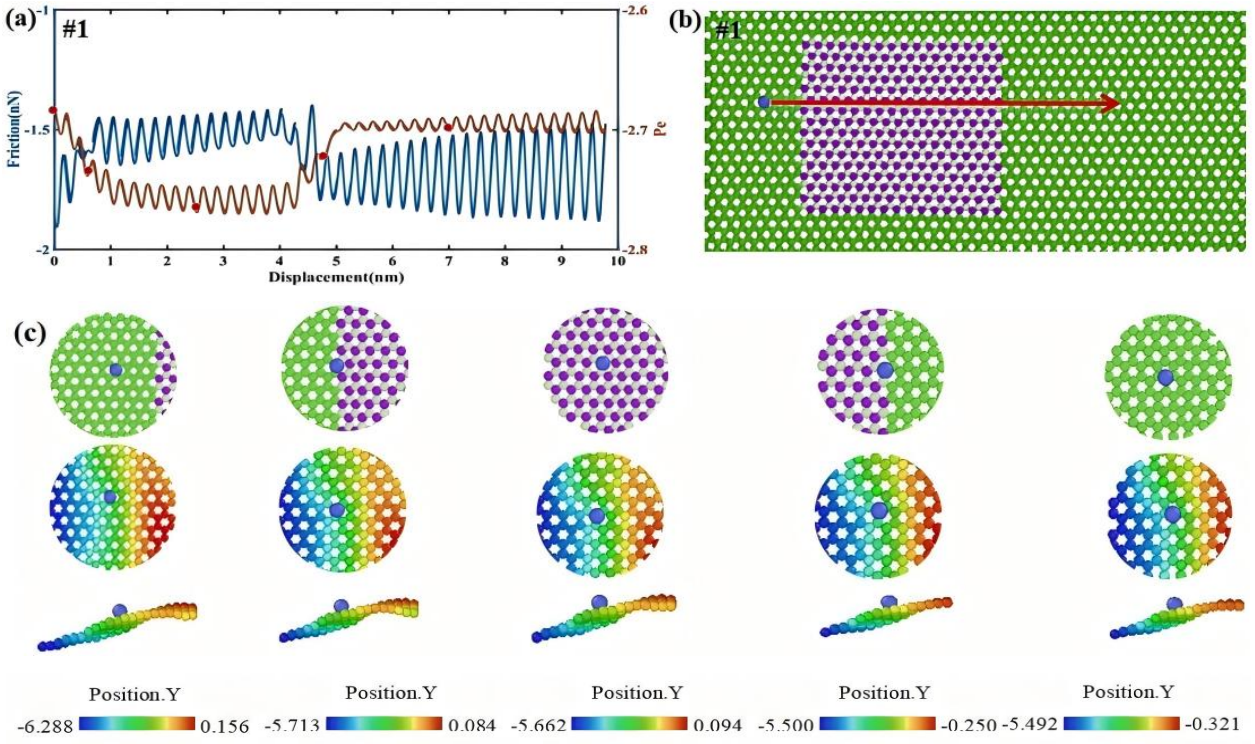

Figure 4. (a) Atomic forces and energy changes of #1 atom in doped system, (b) atomic scanning trajectory of #1 atom in doped system and (c) evolution of graphene deformation around #1atom in doped system

Figure 4(b) shows the trajectory of atom #1 during the scanning process. Five special moments (marked with red dots) are highlighted based on the force change diagram of atom #1, corresponding to different situations of atom #1: (i) not touching the doped area, (ii) about to touch the doped area, (iii) within the doped area, (iv) about to leave the doped area, and (v) far away from the doped area. The graphene interface conditions around it are also shown in Figure 4(c). From the evolution of the interface, it can be seen that when the atoms are in the doped region, the interface wrinkling height is higher than the wrinkling height when the atoms are in the graphene region. When entering the doped region from the graphene region, its out-of-plane deformation increases and remains stable in the doped region. When atoms leave the doped region and enter the graphene region, the interface wrinkling height decreases and the out-of-plane deformation decreases. The reason for this change is that the out-of-plane stiffness of the h-BN region is lower than that of graphene. When the out-of-plane deformation is higher, the interface tends to evolve towards a more asymmetric (lower sliding energy barrier), resulting in a reduction in the atomic forces.

4. CONCLUSION

Based on molecular dynamics (MD) simulation, this study further explored the effect of h-BN doping on the friction behavior and performance of graphene and strived to reveal the physical mechanism behind it. Existing theories believe that the friction force exerted on the indenter mainly comes from the resistance encountered by the outermost atoms in its exclusion area during sliding. Such atoms are called pinning atoms. In the simulation of this study, it was found that on the surface of doped graphene, when the indenter slid from the graphene area to the h-BN doped area, the resistance encountered by the pinned atoms decreased rapidly in a short period of time, and then remained in a relatively constant state until it left the doped area. Correspondingly, the van der Waals potential energy of the pinned atoms changed rapidly from low (more stable strongly aggregated state) to high (less stable weakly aggregated state), and then became basically stable until it was far away from the doped area. In the same process, the resistance and potential energy of the non-pinned atoms on the indenter had no significant change. It can be inferred that the changes in graphene friction behavior and performance caused by doping are all derived from the changes in the friction resistance of the pinned atoms, and these changes originate from the different polymerization states and polymerization strengths of the indenter material, graphene, and h-BN doping.

ACKNOWLEDGEMENTS

This work is supported by the National Natural Science Foundation of China (Grant Nos. 12072134, 12102151, 12350410370), Jiangsu Province Postdoctoral Science Foundation (Grant No. 2021K113B) and Jiangsu Funding Program for Excellent Postdoctoral Talent (Grant No. 2022ZB664).

REFERENCES

[1] Holmberg K, Andersson P and Erdemir A. Global energy consumption due to friction in passenger cars. Tribol Int, Vol. 47, pp. 221-234, 2023. https://doi.org/10.1016/j.triboint.2011.11.022

[2] Hod O, Meyer E, Zheng Q and Urbakh M. Structural superlubricity and ultralow friction across the length scales. Nature, Vol. 563, pp. 485-492, 2018. https://doi.org/10.1038/s41586-018-0704-z

[3] Ge X, Chai Z, Shi Q, Liu Y and Wang W. Graphene superlubricity: a reviewFriction. Volume 11, pp. 1953–1973, 2023. https://doi.org/10.1007/s40544-022-0681-y

[4] Song Y, Mandelli D, Hod O, Urbakh M, Ma M and Zheng Q. Robust microscale superlubricity in graphite/hexagonal boron nitride layered heterojunctions. Nature Mater, Vol. 17, pp. 894-899, 2018. https://doi.org/10.1038/s41563-018-0144-z

[5] Wang D, Chen G, Li Chaokai, et al. Thermally Induced Graphene Rotation on hexagonal boron nitride. Phys Rev Lett, Vol. 116, pp. 126101, 2016. https://doi.org/10.1103/PhysRevLett.116.126101

[6] Zhang Z, Chen C and Guo W. Magnetoelectric effect in graphene nanoribbons on substrates via electric bias control of exchange splitting. Phys Rev Lett, Vol. 103, pp. 187204, 2009. https://doi.org/10.1103/PhysRevLett.103.187204

[7] Hu Z, Zhang Z, Liu L and Guo W. Extreme pseudomagnetic fields in carbon nanocones by simple loads. J Mech. Phys Solids, Vol. 124, pp. 1-9, 2019. https://doi.org/10.1016/j.jmps.2018.09.037

[8] Liu J, Yang X, Fang H, Yan W, Ouyang W and Liu Z. In situ twistronics: a new platform based on superlubricity Adv Mater . https://doi.org/10.1002/adma.202305072

[9] Wu Z, Huang X, Xiang X and Zheng Q. Electro-superlubric springs for continuously tunable resonators and oscillators. Commun Mater. https://doi.org/10.1038/s43246-021-00207-1

[10] Guo W, Bai Q, Dou Y, Chen S and Wang H. Molecular dynamics simulation of frictional strengthening behavior of graphene on stainless steel substrate. Carbon, Vol. 197, pp. 183-191, 2022. https://doi.org/10.1016/j.carbon.2022.06.030

[11] Kawai S, Benassi A, Gencco E, et al. Superlubricity of graphene nanoribbons on gold surfaces. Science, Vol. 351, pp. 957-961, 2016. https://doi.org/10.1126/science.aad3569

[12] Cahangirov S, Ciraci S and Özçelik V O. Superlubricity through graphene multilayers between Ni (111) surfaces Phys Rev B, Vol. 87, pp.205428, 2013. https://doi.org/10.1103/PhysRevB.87.205428

[13] Li P, Ju P, Ji L, Li H, Liu X, Chen L, Zhou H and Chen J. Toward robust macroscale superlubricity on engineering steel substrate. Adv Mater, Vol. 32, pp.18-24, 2020. https://doi.org/10.1002/adma.202002039

[14] Huang X, Li T, Wang J, Xia K, Tan Z, Peng D, Xiang X, Liu B, Ma M and Zheng Q. Robust microscale structural superlubricity between graphite and nanostructured surface. Nat Commun, Vol. 14, pp.2931, 2023. https://doi.org/10.1038/s41467-023-38680-6

[15] Liu S W, Wang H P, Xu Q, et al. Robust microscale superlubricity under high contact pressure enabled by graphene-coated microsphere. Nature Communications, Vol. 8, pp.14029, 2017. https://doi.org/10.1038/ncomms14029

[16] Leven I, Krepel D, Shemesh O, et al. Robust Superlubricity in Graphene/h-BN Heterojunctions. Physical Chemiacl Letters, Vol. 4, pp.115-120, 2012. https://doi.org/10.1021/jz301758c

[17] Nataly H R, Alisson C D S, Luis H D L, et al. Atomically Precise Bottom-Up Synthesis of h-BNC: Graphene Dopedwith h-BN Nanoclusters. Chemistry of Materials, Vol. 33, pp.2871-2882, 2021. https://doi.org/10.1021/acs.chemmater.1c00081

[18] Uddin M R, Li J, Lin J Y, et al. Carbon-rich hexagonal (BN) C alloys. Journal of Applied Physics, Vol. 117, pp.215703, 2015. https://doi.org/10.1063/1.4921931

[19] Fiori G, Betti A, Bruzzone S, et al. Lateral Graphene-hBCN Heterostructures as a Platform for Fully Two Dimensional Transistors. American Chemical Society Nano, Vol. 6, pp.2642-2648, 2012. https://doi.org/10.1021/nn300019b

[20] Alcaraz Iranzo D, Nanot S, Dias E J C, et al. Probing the ultimate plasmon confinement limits with a van der Waals heterostructure. Science, Vol. 360, pp. 291-295, 2018. https://doi.org/10.1126/science.aar8438

[21] Li M, Wang Y, Tang P, et al. Graphene with Atomic Level In-Plane Decoration of h-BN Domains for Efficient Photocatalysis. Chemistry of Materials, Vol. 29, pp. 2769-2776, 2017. https://doi.org/10.1021/acs.chemmater.6b04622

[22] Chen S, Li P, Xu S, et al. Carbon doping of hexagonal boron nitride porous materials toward CO2 capture. Journal of Materials Chemistry A, Vol. 6, pp. 1832-1839, 2018. https://doi.org/10.1039/C7TA08515J

[23] Wang S, Ma F, Jiang H, et al. Band gap Tunable Porous Boro carbonitride Nanosheets for High Energy Density Supercapacitors. ACS Applied Materials & Interfaces, Vol. 10, pp. 19588-19597, 2018. https://doi.org/10.1021/acsami.8b02317

[24] Li S, Li Q, Carpick R W, et al. The evolving quality of frictional contact with graphene. Nature, Vol. 539, pp. 541-545, 2016. https://doi.org/10.1038/nature20135